HDL Mimetic Peptide ATI-5261 Forms an Oligomeric Assembly in Solution That Dissociates to Monomers upon Dilution

Ying Zheng,[†,⊥] Arti B. Patel,[‡,⊥] Vasanthy Narayanaswami,[‡,§] Gregory L. Hura,[∥] Bo Hang,[†] and John K. Bielicki*,[†]

[†]Life Sciences Division, Lawrence Berkeley National Laboratory, Donner Laboratory, University of California, Berkeley, Berkeley, California 94720, United States

[‡]Department of Chemistry and Biochemistry, California State University, Long Beach, California 90840, United States

[§]Children's Hospital of Oakland Research Institute, Oakland, California 94609, United States

[∥]Physical Biosciences Division, Lawrence Berkeley National Laboratory, Berkeley, California 94720, United States

ABSTRACT: ATI-5261 is a 26-mer peptide that stimulates cellular cholesterol efflux with high potency. This peptide displays high aqueous solubility, despite having amphipathic α-helix structure and a broad nonpolar surface. These features suggested to us that ATI-5261 may adopt a specific form in solution, having favorable structural characteristics and dynamics. To test this, we subjected ATI-5261 to a series of biophysical studies and correlated self-association with secondary structure and activity. Gel-filtration chromatography and native gel electrophoresis indicated ATI-5261 adopted a discrete self-associated form of low molecular weight at concentrations >1 mg/mL. Formation of a discrete molecular species was verified by small-angle X-ray scattering (SAXS), which further revealed the peptide formed a tetrameric assembly having an elongated shape and hollow central core. This assembly dissociated to individual peptide strands upon dilution to concentrations required for promoting high-affinity cholesterol efflux from cells. Moreover, the α-helical content of ATI-5261 was exceptionally high (74.1 ± 6.8%) regardless of physical form and concentration. Collectively, these results indicate ATI-5261 displays oligomeric behavior generally similar to native apolipoproteins and dissociates to monomers of high α-helical content upon dilution. Optimizing self-association behavior and secondary structure may prove useful for improving the translatability and efficacy of apolipoprotein mimetic peptides.
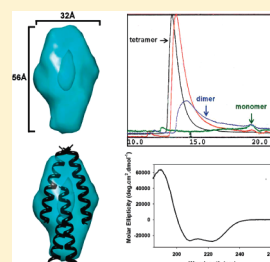
Plasma apolipoproteins play diverse roles in biology and medicine, including the development of atherosclerosis.[1−10] Members of this protein family can be found associated with lipoproteins in blood and play prominent roles in lipid metabolism as well as anti-inflammatory processes. Their broad biological importance is underscored by expanding roles in diabetes, neurobiology, blood coagulation, and host defense, suggesting apolipoproteins may be useful for diagnostic and therapeutic applications in a variety of disease settings.

Apolipoprotein (apo)A-I is the most abundant protein of HDL and is thought to protect against atherosclerosis.[11−14] Apolipoprotein E found in VLDL, chylomicrons, and HDL and is also considered antiatherogenic.[15−17] The beneficial effects of apoA-I and E are generally related, in part, to activity in mediating reverse cholesterol transport (RCT).[18−23] This process involves removal of excess cholesterol from macrophage foam cells in arterial plaque followed by the transport of cholesterol to the liver for excretion in feces. ApoE also mediates lipid transport in the brain and is considered a major risk factor for Alzheimer's disease.[10,24−26] Despite therapeutic potential,[27−32] there is uncertainty whether full-length apolipoproteins will be suitable for widespread clinical applications. Recombinant proteins are generally costly to manufacture and chemically complex, posing formidable challenges with regards to formulation and stability.

Small peptides represent an attractive alternative to proteins for routine use. However, designing peptides based on the plasma apolipoproteins is not without difficulties. Apolipoproteins generally consist of a series of amphipathic α-helices. Often several of these α-helices linked via proline are required to support potent biological activity.[33−36] As a result, short sequences taken directly from native proteins typically possess poor structure and activity.[33,36,37] Poor structure can predispose to peptide aggregation via nonspecific hydrophobic interactions, thereby decreasing solubility.[37,38] These problems complicate production/purification, limit biological applications, and confound interpretations of experimental results.

Recently, we designed an apolipoprotein mimetic peptide (ATI-5261) that displays hydrophobic character as well as potent cholesterol efflux and lipid binding activities.[39] These features together with its high aqueous solubility suggested to us that ATI-5261 may possess favorable structural characteristics in solution. Therefore, we tested whether ATI-5261 adopted a discrete molecular form at high concentrations, as suggested by its high aqueous solubility. We also sought to determine whether specific self-associated species were seen at low concentrations, which correlated with secondary structure and activity. We found that ATI-5261

formed a unique assembly of four noncovalently bound α-helical strands that dissociated to trimers, dimers, and monomers in a concentration-dependent manner, similar to that reported for apoA-I.[40,41] Moreover, ATI-5261 retained high α-helical content upon extensive dilution, regardless of specific self-associated form. The data suggest ATI-5261 constitutes a new model for indentifying factors to improve structure and activity of HDL mimetic therapies.

■ EXPERIMENTAL PROCEDURES

Peptides. Peptides were synthesized (Biosynthesis Inc., Lewisville, TX) using all L-amino acids, capped with N-terminal acetyl and C-terminal amide groups, isolated by HPLC and used at a purity of >95%. The sequence EVRSKLEEWFAAFREFAEE-FLARLKS corresponded to that of ATI-5261 and DWFKAFYDK-VAEKFKEAF peptide 4F.[38] Peptide 4F was used as a positive control (where applicable) because it represents a prototypical class A consensus peptide, and its biophysical properties[42,43] have been characterized. Unless otherwise stated, lyophilized peptides were dissolved in 10 mM phosphate buffered (pH = 7.4) saline (150 mM NaCl), referred to as PBS. Peptide concentrations were determined by absorbance at 280 nm.

Self-Association Properties of Peptides. Nondenaturing gradient gel electrophoresis was performed using premade Novex 4—20% Tris-Glycine gels (Invitrogen). Gels were stained with SimplyBlue SafeStain (Invitrogen) and destained with distilled water to visualize peptides. Distribution of ATI-5261 physical forms was evaluated by fast protein liquid chromatography (FPLC), using either Superdex 75 10/300GL or Superdex peptide columns (GE Healthcare) pre-equilibrated with PBS. The system was operated at a flow rate of 0.5 mL/min at room temperature and 0.2 mL of peptide stock solutions injected onto columns. Elution of peptides was monitored by either 280 or 215 nm absorbance using a UVis920 GE detector. No differences were noted in ability of ATI-5261 to adopt a single self-associated species when FPLC experiments were performed at room temperature versus 4 °C (data not shown). Columns were calibrated with the appropriate molecular weight standards indicated by the manufacturer and shown in figure legends.

Small-angle X-ray scattering (SAXS) was used to verify the size and oligomeric status of ATI-5261 in solution. X-ray scattering data were collected at SIBYLS[44] (beamline 12.3.1, sibyls.als.lbl.gov) at the Advanced Light Source, Lawrence Berkeley National Laboratory. 15 μL of each of three concentrations of ATI-5261 and matching buffer (PBS) were used for collecting scattering data at 20 °C. Shape was determined by the program GASBOR.[45] Ten individual and highly consistent GASBOR runs were averaged to determine the final shape of the ATI-5261 assembly. Two independent preparations of ATI-5261 yielded identical results.

DMS Cross-Linking of ATI-5261. Cross-linking of ATI-5261 was achieved with dimethyl suberimidate (DMS, Pierce Biotechnolgy, Rockford, IL), dissolved in 0.2 M triethanolamine, pH = 8.0. Peptide samples were reacted with 20-fold molar excess of DMS for 3 h at 25 °C. The reaction was terminated by addition of 50 mM Tris-HCl. Reaction products were mixed with 3× SDS loading buffer (Cell Signaling Technology, Inc.) and then boiled for 1 min. The supernatants were loaded onto a 10—20% Tris-Tricine SDS-PAGE gel and electrophoresed. Spectra Multicolor Low Range Protein standards (1.7—40 kDa, Fermentas) were used to identify the size of cross-linked species, visualized with SimplyBlue SafeStain. A substantial number of studies were performed to ensure optimal conditions were used to produce maximal cross-linking of peptide samples. These experiments included variation of incubation time
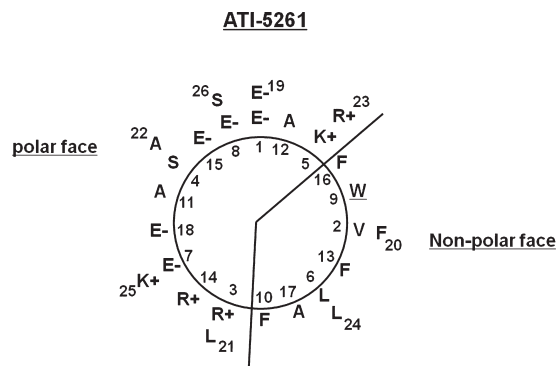

Figure 1. Helical-wheel projection of ATI-5261. Linear sequence of amino acids is denoted by numbers, beginning with residue 1 in the intended foreground. Cationic residues are found at the polar/nonpolar interface and negatively charged amino acids down the center of the polar surface, characteristic of a class A α-helix. A single tryptophan (W) residue is located on the nonpolar surface.

and concentration of DMS as well as use of alternative cross-linking reagents. The latter included use of glutaraldehyde and acrolein, which produced essentially identical results as those obtained with DMS (data not shown).

CD Spectroscopy. Circular dichroism (CD) spectroscopy was carried out on a Jasco 810 spectropolarimeter at 25 °C, using lipid-free peptide in 10 mM sodium phosphate buffer (pH = 7.4) and averaging 4 scans (20 nm/min/scan) per peptide per run (i.e., each concentration) as described.[46]

Fluorescence Spectroscopy. Fluorescence emission spectra of ATI-5261 (1 mg/mL) in the presence/absence of 50% trifluoroethanol (TFE) in sodium phosphate buffer, pH = 7.4, were recorded at 25 °C. The Trp fluorescence emission was monitored following excitation at 280 nm and was recorded between 300 and 500 nm on a PerkinElmer spectrofluorimeter. A blank of buffer alone was subtracted from all spectra.

Cell Culture and Cholesterol Efflux Assay. J774 mouse macrophages were grown in RPMI-1640 medium supplemented with 10% fetal bovine serum (FBS). Cells were plated onto 24-well culture plates and labeled with [³H]cholesterol (1 μCi/mL) in RPMI-1640 with 1% FBS for 48 h. A cAMP analogue (cpt-cAMP) was added (final concentration of 0.3 mM) to upregulate ABCA1 expression. Cells were extensively rinsed with serum-free RPMI-1640 medium followed by an extended rinse (2 h) with RPMI-1640 containing 0.2% bovine serum albumin (BSA). Lipid-free peptides were added to cells in serum-free RPMI-1640 medium to initiate cholesterol efflux. The amount of [³H]cholesterol appearing in the medium was expressed as a percentage of the radioactivity initially present in cells at time zero.[47] The background release of [³H]cholesterol to serum-free medium alone was subtracted from the values obtained with lipid-free peptides.

Lipid Clearance Assay. A turbid solution of dimyristoylphosphatidylcholine (DMPC) was used to assess relative capacity of peptides to solubilize phospholipid.[47] The DMPC was used at a final concentration of 0.16 mg/mL PBS (pH = 7.4). The mass ratio of DMPC to peptides was 2:1 or 4:1. The absorbance (400 nm) of samples was monitored continuously over a period of 20 min at 25 °C.

Statistics. Where appropriate, data were expressed as means ± SD of at least three independent experiments and statistical analyses performed using Student's t-test.
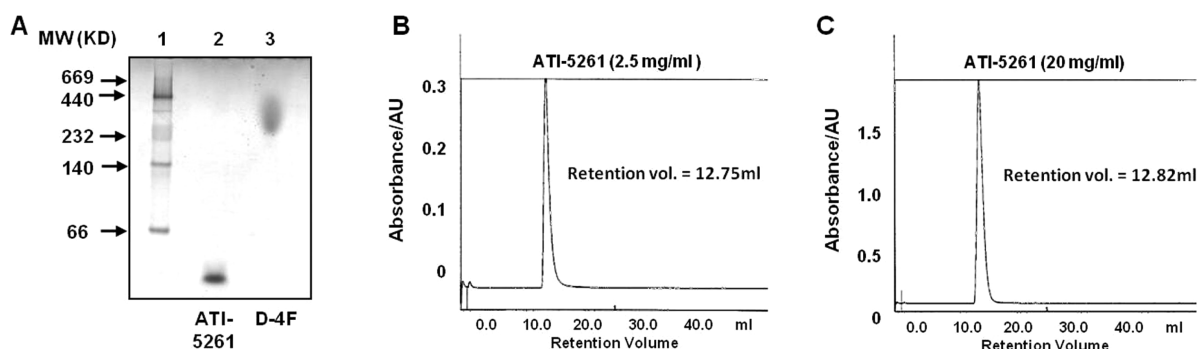
Figure 2. ATI-5261 adopts a low molecular weight form in aqueous buffer. Stock solutions of ATI-5261 and peptide 4F were prepared in PBS (pH = 7.4). (A) Native-PAGE (4–20% Tris-Glycine gel) of peptides taken from 1 mg/mL stock solutions: lane 1, mobility of molecular weight (MW) standards including thyroglobulin (669 kDa), ferritin (440 kDa), catalase (232 kDa), lactate dehydrogenase (140 kDa), and albumin (66 kDa); lane 2, ATI-5261; lane 3, 4F. Peptide loads were 3 μg per well. Panels B and C: chromatographic behavior of ATI-5261 in PBS on Superdex 75 columns at a flow rate of 0.5 mL/min. Peptide elution was monitored by absorbance at 280 nm. Representative profiles are shown for stock solution of 2.5 (B) and 20 mg/mL (C).
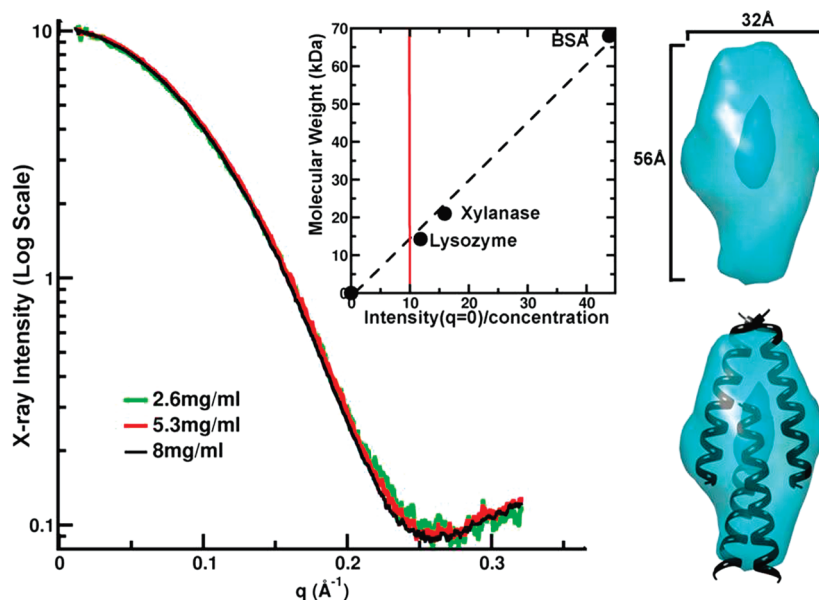

Figure 3. Small-angle X-ray scattering (SAXS) reveals ATI-5261 forms a tetrameric assembly. Peptide stock solutions were prepared in PBS (pH = 7.4). X-ray scattering curves for ATI-5261 at three concentrations are shown. Once scaled for concentration, the X-ray intensity at $q = 0$ (inset, red line) was determined to be 13.1 kDa or 4.1 times the monomeric weight of the peptide when calibrated against molecular weight standards lysozyme, xylanase, and BSA. The elongated shape determined from the SAXS curves (teal) has a hollow central core. Picture at bottom right shows hypothetical fit of 4 α-helical strands within volume estimates, illustrating how overlapping segments may account for the elongated shape of the assembly.

■ RESULTS

ATI-5261 is composed of a linear sequence of 26 amino acids that form a class A amphipathic α-helix with opposing polar and nonpolar surfaces (Figure 1). The amphipathic nature of the peptide suggests it may self-associate to shield hydrophobic residues from water. Therefore, we performed a series of biophysical studies to evaluate the oligomeric behavior of the peptide in solution. ATI-5261 migrated as a low molecular weight (LMW) band on nondenaturing gels (Figure 2A). This contrasted the behavior of peptide 4F, which aggregated as high molecular weight (HMW) species under identical conditions, i.e., stock solutions = 1 mg/mL PBS, pH = 7.4.

A single sharp peak of ATI-5261 was consistently obtained by gel-filtration chromatography, using a Pharmacia FPLC system fitted with a Superdex 75 column (Figure 2B). Elution profiles and retention volumes (12.8 mL) were identical using ATI-5261 from stock solutions of either 2.5 or 20 mg peptide/mL (Figure 2B,C). Similar results were also obtained using stock solutions of 140 mg peptide/mL (highest concentration tested), indicating ATI-5261 adopted a relatively consistent and stable form over a wide range of concentrations with little or no apparent aggregation tendency. Similarly, gel filtration profiles were not altered by prolonged storage (2 years) in PBS at 4 °C under sterile conditions or following incubation at 37 °C for 24 h (data not shown). In contrast, peptide 4F could not be resolved on the Superdex 75 column and typically eluted with extensive rinsing and/or with 0.5 N NaOH, consistent with its tendency to form HMW aggregates as shown on native PAGE (Figure 2A).

The ability of ATI-5261 to maintain a constant physical form over a broad range of concentrations (>1 mg/mL) suggested the peptide may form a discrete structure in solution. This was
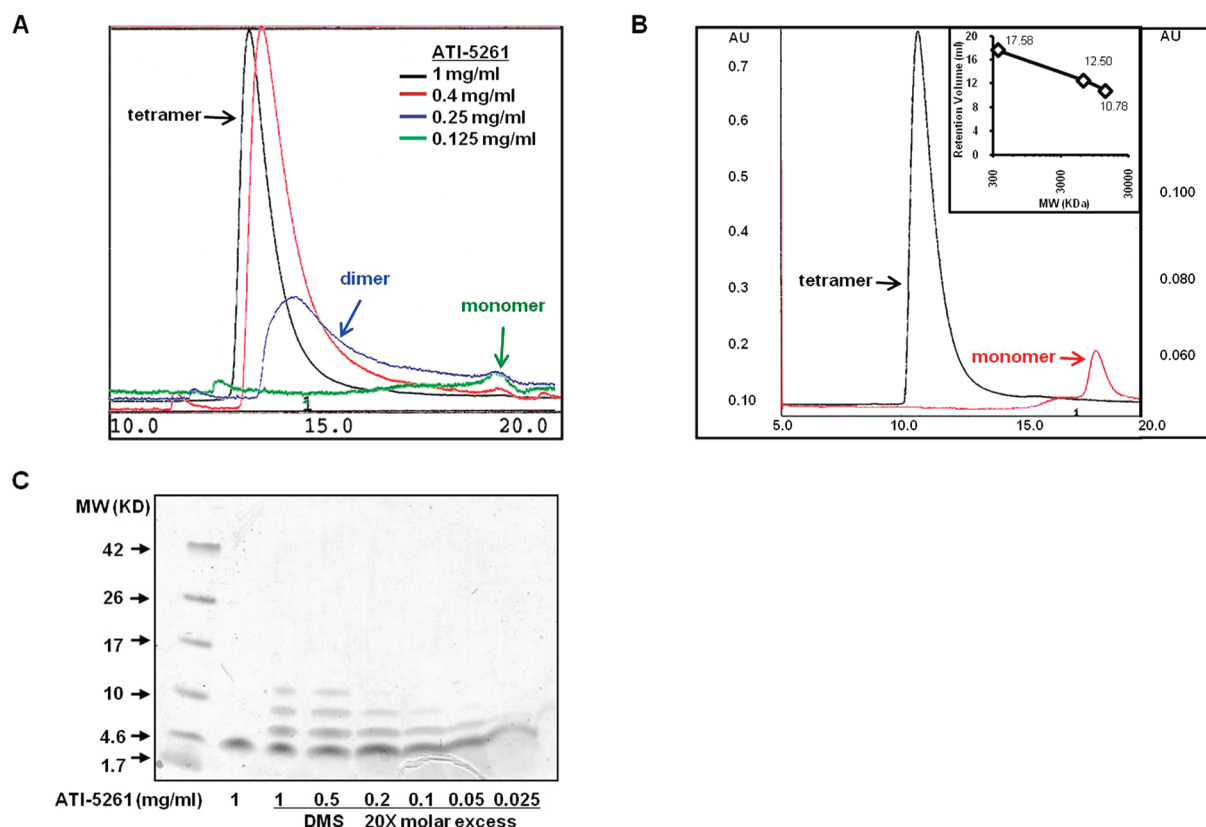
Figure 4. Tetrameric assembly of ATI-5261 dissociates to lower molecular weight forms upon dilution. Stock solution of ATI-5261 prepared in PBS (pH = 7.4) were analyzed by gel-filtration chromatography. Panel A: separation of various physical forms of ATI-5261 on a Superdex 75 column; 0.2 mL of each stock solution (indicated) was injected onto the column; flow rate was 0.5 mL/min; elution buffer was PBS. Representative chromatographic profiles of ATI-5261 stock solutions: 1 mg/mL (black), 0.4 mg/mL (red), 0.25 mg/mL (blue), and 0.125 mg/mL (green) are shown. Elution was monitored using absorbance at 280 nm. Results are arbitrary absorbance units (AU) scaled to clearly illustrate peak positions; actual AU = 1.0, 0.25, 0.08, and 0.02 for stock solutions of 1, 0.4, 0.25, 0.125 mg ATI-5261/mL, respectively. Panel B: FPLC using Superdex Peptide 10/300 GL columns to separate ATI-5261 forms. Representative profiles of ATI-5261 at 1 mg/mL (black) and 0.1 mg/mL (red) are shown. Calibration curve (inset) shows retention volume of 17.58 mL for $(Gly)_6$ (0.36 kDa), 12.5 mL for aprotinin (6.5 kDa) and 10.78 mL for ribonuclease A (13.6 kDa). Elution was monitored by absorbance at 215 nm. Panel C: ATI-5261 at various concentrations cross-linked with DMS and separated by SDS-PAGE (10−20% Tricine Gel). Cross-linking patterns were visualized by staining with SimplyBlue SafeStain.

evaluated by small-angle X-ray scattering (Figure 3). Little or no aggregation was detected from the X-ray intensity profiles using peptide at 2−8 mg/mL PBS, consistent with results obtained by gel-filtration chromatography (Figure 2). Thus, the X-ray scattering curves for ATI-5261 were highly reproducible over the concentration range examined, yielding an estimated MW of 13 kDa. This corresponded to nearly 4 times the MW (3230 Da) of monomeric peptide. Scattering curves also revealed the ATI-5261 tetramer displayed an elongated shape (height/width ratio of 1.75) and hollow central region. These results suggest inter-helical interactions were greater toward the ends of the assembly. Peptide 4F failed to meet the acceptance criteria for SAXS analysis at the advanced light source LBNL because the solubility was too low in PBS (maximum solubility was ∼1 mg/mL) and because we could not detect a single homogeneous peak by FPLC (http://bl1231.als.lbl.gov/saxs_protocols/saxs_sample_prep.php).

More detailed FPLC experiments were conducted to determine if the ATI-5261 assembly remained intact upon extensive dilution or whether the complex dissociated to individual peptide strands, as concentrations approached the active biological range.[39] A characteristic peak (retention volume = 12.8 mL)

corresponding to the ATI-5261 tetramer was observed using stock solutions of 1 mg peptide/mL (Figure 4A). Dilution of peptide to 0.25 mg/mL produced a broad peak on the Superdex 75 column, corresponding to a heterogeneous mixture of various low molecular weight species, whereas more extensive dilutions (<0.25 mg/mL) mostly monomeric peptide (Figure 4A). The latter was verified using a high resolution Superdex peptide column (Figure 4B). Moreover, the MW (12.8 kDa) of the peptide assembly was found to be identical to that revealed by SAXS, i.e., using 1 mg peptide/mL (Figure 4B). Close examination of the FPLC profiles (base width) and consideration of injection volume (0.2 mL) suggest ATI-5261 is subjected to ∼10-fold dilution on the columns, indicating peptide monomers were predominant at concentrations <0.025 mg/mL. This was verified by SDS-PAGE/chemical cross-linking assay, which revealed dissociation of the tetrameric assembly to monomers at 0.5−0.025 mg/mL concentrations (Figure 4C). Collectively, these results indicate the ATI-5261 assembly dissociates to peptide monomers at low concentrations, where the cholesterol efflux response is sensitive to peptide concentration in the extracellular medium.[39]

Figure 5A shows a representative CD scan of ATI-5261 in 10 mM phosphate buffer (pH = 7.4). The lipid-free peptide
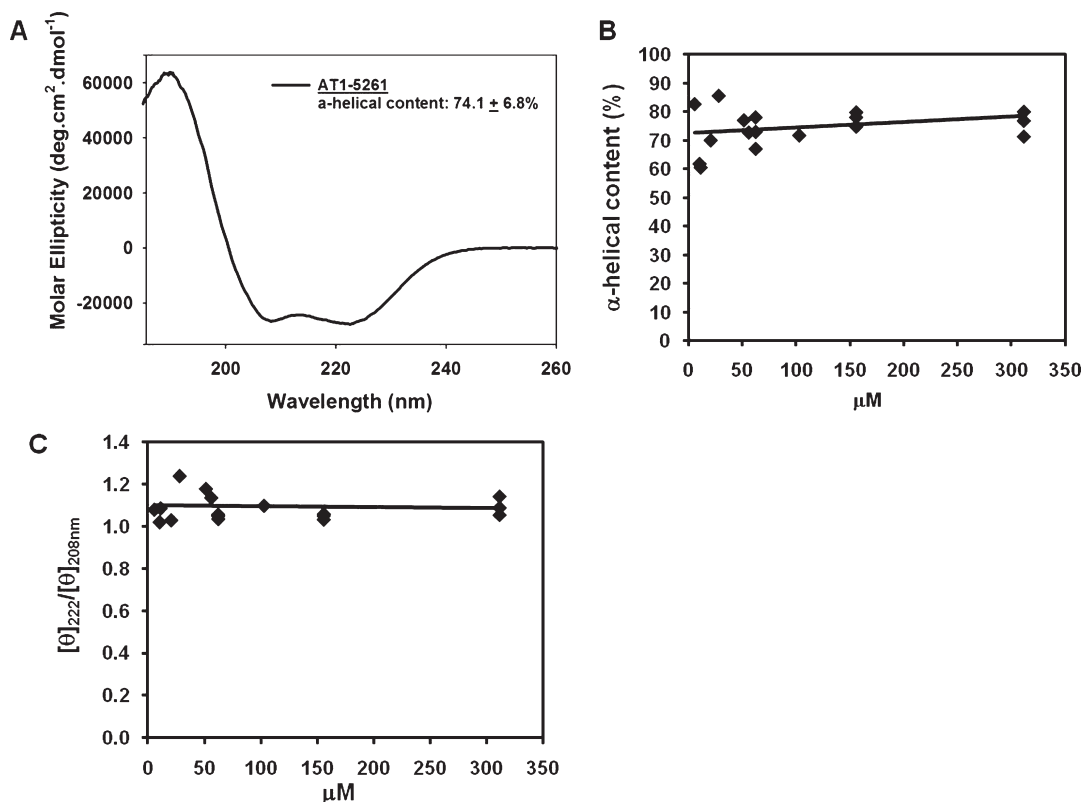
Figure 5. ATI-5261 maintains high α-helical content and structural integrity over a wide range of concentrations. Peptide stock solutions of 2 mg/mL were prepared in 10 mM phosphate buffer (pH = 7.4) and diluted with this same buffer as indicated. Panel A: representative circular dichroism (CD) spectrum of lipid-free ATI-5261 at a concentration of 0.2 mg/mL (62 μM) is shown. Mean α-helicity was calculated from the molar ellipticity at 222 nm ($n = 4$). Panel B: α-helical content of ATI-5261 at various concentrations, ranging from 6 to 310 μM (18−1000 μg/mL). Panel C: molar ellipticity ratio ($[\theta]_{222}/[\theta]_{208}$) plotted against concentration of ATI-5261.

possessed high α-helical content (74.1 $\pm$ 6.8%), as judged by molar ellipticity at 222 nm. Moreover, α-helical content remained relatively constant over a wide range of peptide concentrations (6−310 μM, i.e., 18−1000 μg/mL), indicating ATI-5261 exhibited a strong propensity to form an α-helix (Figure 5B). CD scans were further characterized by a prominent peak at 208 nm of equivalent ellipticity to the 222 nm peak (Figure 5A). This pattern (222/208 ellipticity ratio) also remained constant with increasing peptide concentrations, indicating secondary structure was well maintained (Figure 5C). The latter was particularly noted for extensively diluted samples (6 μM, i.e., 18 μg/mL of ATI-5261), wherein α-helical content remained relatively high (82.6%). The C-terminal (CT) domain of apoE, from which ATI-5261 was derived, also possessed relatively high α-helical content (65% and 68%, two separate experiments at 0.1 mg/mL concentration) that similarly remained constant upon dilution, as described.[48,49]

Treatment with the membrane mimetic trifloroethanol (TFE) had little impact of peptide secondary structure, as α-helical content remained unchanged by the presence of 50% TFE compared to controls with no TFE (Figure 6A,B). However, TFE markedly increased the 208 nm molar ellipticity of ATI-5261, and hence, the 222/208 ellipticity ratio was <1. This behavior is consistent with formation of single-stranded α-helix and generally mimics the behavior of apoE CT domain.[48] Disruption of strand−strand interactions was verified by SDS-PAGE/chemical cross-linking assay, which demonstrated 50% TFE was sufficient to produce mostly monomeric peptide

(Figure 6C). The latter was accompanied by a marked decrease in tryptophan fluorescence intensity, accompanied by a 2 or 3 nm shift in the wavelength of maximal fluorescence emission toward higher wavelengths with 50% TFE, reflecting exposure of the nonpolar surface of the peptide to the aqueous environment (Figure 6D). In contrast, the α-helical content of peptide 4F was generally low at 0.2 mg/mL but was greatly enhanced upon addition of 50% TFE (28% vs 49%, absence and presence of 50% TFE, respectively), consistent with the known behavior of the peptide.[50]

To determine whether the high α-helical content of ATI-5261 was related to end-group blockage, the peptide was synthesized with and without N-terminal acetyl and C-terminal amide groups. ATI-5261 lacking end-group modifications retained high (56.9 $\pm$ 0.8%) α-helical content over the experimental range of concentrations, indicating secondary structure was minimally dependent on the end-group modifications (Figure 7A,B). Moreover, ATI-5261 lacking end-group modifications retained selective and potent cholesterol efflux activity (Figure 7C,D) as well as the ability to bind phospholipid (Figure 7, E vs F). These results suggest secondary structure and activity of ATI-5261 are largely dependent on intrinsic properties of the peptide and, thus, minimally impacted by end-group modification.

■ DISCUSSION

Recently, we created a single α-helix peptide designated ATI-5261 that stimulates cellular cholesterol efflux with
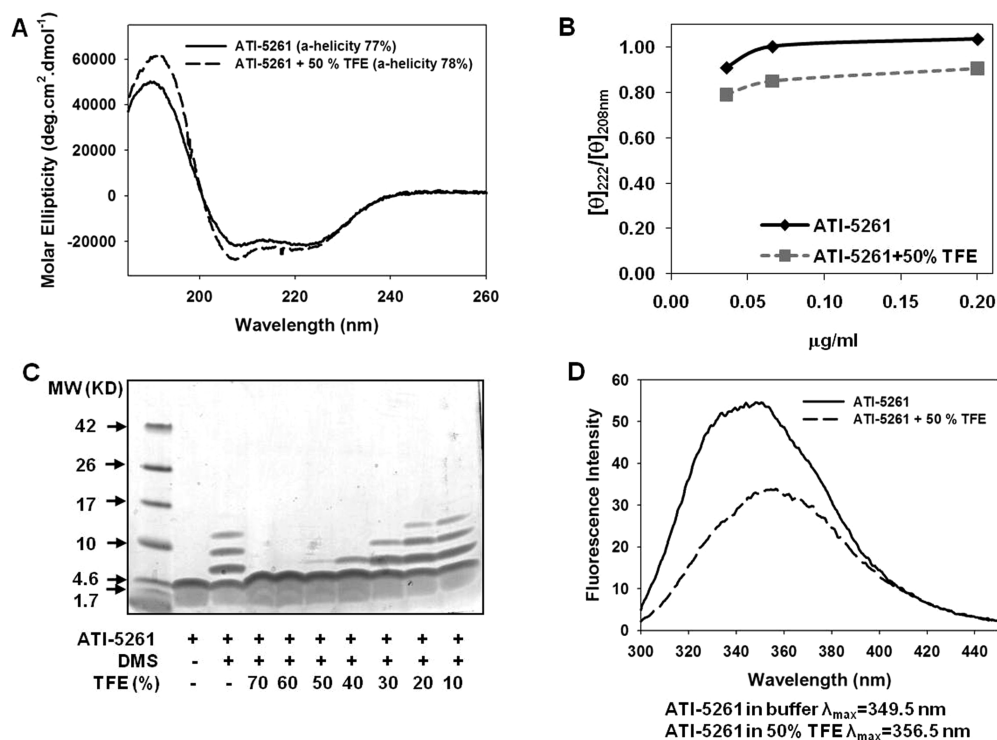
Figure 6. Effect of membrane mimetic trifluoroethanol (TFE) on self-association and secondary structure of ATI-5261. Stock solution of ATI-5261 were prepared in 10 mM phosphate (pH = 7.4) and treated with and without TFE for 30 min at 25 °C before analysis. Panel A: CD spectra of lipid-free ATI-5261 (0.2 mg/mL) in the presence or absence of 50% TFE, showing mean α-helicity calculated from molar ellipticity at 222 nm ($n = 3$). Panel B: $[\theta]_{222}/[\theta]_{208}$ ratio of ATI-5261 in the presence and absence of 50% TFE, plotted against concentration of peptide. Panel C: DMS cross-linking/SDS-PAGE of ATI-5261 following treatment (30 min) with increasing amounts of TFE. A representative stained gel is shown, indicating predominantly monomeric peptide at concentrations >40% TFE. Panel D: fluorescence emission spectra of ATI-5261 in the presence or absence of 50% TFE. Results are representative of three separate experiments with different batches of peptide.

apolipoprotein molar potency.[39] This peptide is unique because previous studies have suggested several α-helical segments linked via proline are required for mediating cholesterol efflux efficiently via ABCA1.[33−35] Potent activity coupled with high aqueous solubility suggested to us that ATI-5261 may possess favorable structural features. Thus, we evaluated biophysical properties of ATI-5261 to better understand peptide structure and activity. We found that ATI-5261 (a) formed a discrete assembly of four noncovalently bound α-helices with little or no tendency to aggregate as high molecular weight species, (b) dissociated to trimers, dimers, and monomers upon extensive dilution, and (c) retained high α-helical content regardless of concentration, specific self-associated form, presence of N- and C-terminal capping, and stabilizing agent TFE. These features distinguish ATI-5261 from other apolipoproteins mimetics in the literature, indicating the peptide constitutes a new platform for studies of α-helix structure and for optimizing the biophysical properties of HDL mimetic therapies.

Nonspecific aggregation of peptides generally produces high molecular weight forms with limited solubility.[38] This can create difficulties when using peptides and confound interpretations of experimental results, thereby hindering scientific and clinical applications. In contrast, ATI-5261 readily formed a single low molecular weight (LMW) species over a broad-range of concentrations ≥1 mg/mL, as determined by FPLC using a Superdex 75 column. Similar results were consistently seen using a high resolution Superdex Peptide column, which revealed ATI-5261 exhibited an apparent molecular weight (∼12.8 kDa) roughly

4 times the size of the monomeric peptide (MW = 3230). Formation of single LMW species was verified by SAXS. These analyses employed peptide at concentrations (2−8 mg/mL) that overlapped FPLC experiments using ATI-5261 ≥ 1 mg/mL. This behavior to adopt a tetrameric form likely accounts for the high aqueous solubility of ATI-5261 in the absence of lipid, providing favorable solution properties in physiological buffers with little or no apparent aggregation tendency.

To our knowledge, ATI-5261 is the first HDL/apolipoprotein mimetic amenable to high-resolution structural analysis in the absence of lipid. Such studies may prove useful for identifying determinants that control peptide aggregation and solubility as well as new features not yet considered to optimize structure/activity of HDL mimetics. This is made possible because of the uniform nature of the ATI-5261 self-associated form, which provides a highly homogeneous sample for detailed analysis. The present studies employing SAXS offers an example of this, where 15−20 Å resolution of ATI-5261 assembly was achieved. This technique revealed ATI-5261 formed a tetrameric assembly of elongated shape under physiological conditions of salt and pH. Formation of a tetrameric assembly was generally consistent with various cross-linked forms generated upon exposure to DMS. These cross-linked forms ranged in size from monomers to tetramers and likely reflect overlapping peptide strands characteristic of the assembly predicted by SAXS. These assertions are based on the height/width ratio of 1.75 for the assembly as well as the length (56 Å) of its long-axis, which is considerably greater than that predicted (32 Å) for single stranded peptide of 7 helical
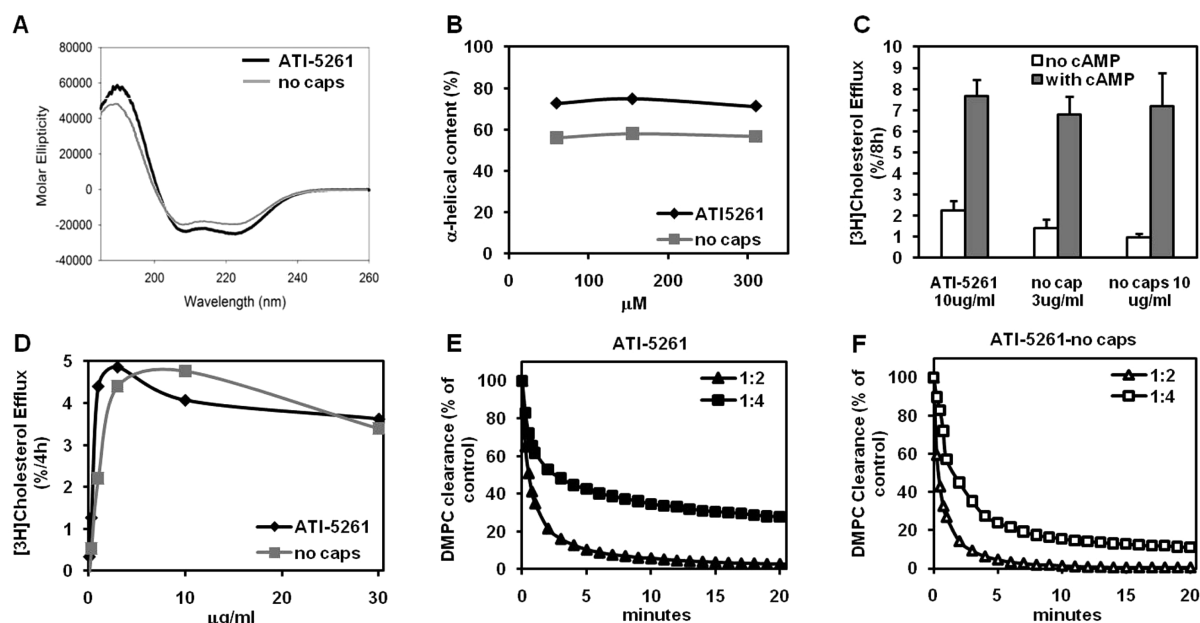
Figure 7. Impact of end-group modifications on secondary structure, cholesterol efflux, and lipid binding activities of ATI-5261. ATI-5261 was synthesized with and without N-terminal acetyl and C-terminal amide groups and dissolved in 10 mM phosphate buffer (pH = 7.4). Panel A: representative CD scan and mean α-helicity of ATI-5261 (62 μM) lacking end-group modifications. Panel B: relationship between α-helicity and concentration of ATI-5261 with and without end-group modifications. Panel C: ability of ATI-5261 to promote cholesterol efflux from J774 macrophages treated with and without cAMP. Cells labeled with [^{3}H]cholesterol were incubated (4 h) with lipid-free ATI-5261 and ATI-5261 lacking end-group modifications (3 μg/mL each) to monitor cholesterol efflux. Values are means ± SD, $n = 5$. Panel D: dependence of cholesterol efflux on the concentration of lipid-free ATI-5261 with/without end-group modifications, determined using J774 cells treated with cAMP. Results are representative of two experiments. Panel E: lipid-binding activity of ATI-5261, prepared with N-terminal acetyl and C-terminal amide groups. Lipid-binding activity was assessed as clearance of turbid solutions of DMPC, using peptide:lipid mass ratios of 1:2 and 1:4 at 25 °C and following absorbance at 400 nm. Panel F: lipid-binding activity of ATI-5261, lacking end-group modifications; conditions identical to panel E. Results are representative of two separate experiments.

turns (i.e., 26-mer peptide of high α-helical content). Exposure of ATI-5261 to 50% TFE produced monomeric peptide with concomitant quenching of tryptophan fluorescence. This reflects exposure of the nonpolar surface to water upon dissociation of the assembly and suggests ATI-5261 self-associates via interactions between nonpolar surfaces of adjacent helical strands, thereby shielding hydrophobic amino acids from the bulk water phase. Such a mechanism would be consistent with the peptide's high solubility, maximizing exposure of polar residues to the aqueous environment.

ATI-5261 stimulates cellular cholesterol efflux with a K_m = 0.86 μg/mL (0.27 μM), displaying saturation in efflux at 3 μg/mL. Presently, we found that the ATI-5261 tetramer dissociated to lower molecular weight species upon dilution, in keeping with studies of native apolipoproteins.[40,41,51] This was verified by FPLC using Superdex 75 and Peptide columns as well as SDS-PAGE/chemical cross-linking assays with DMS, visualizing peptide with a stain (Figure 4). These techniques revealed that monomeric ATI-5261 predominated at concentrations ≤25 μg/mL, i.e., far above the concentration required for mediating cholesterol efflux efficiently. Therefore, we believe activity of the peptide may be attributed to its lower molecular weight forms, reflecting dissociation of "inactive" tetramers to expose nonpolar surfaces for binding lipid.

The α-helical content of apoA-I mimetic peptides is generally thought to increase with increasing peptide concentration, indicating helix—helix interactions can induce α-helical formation/stability.[50] Results presented in Figure 5 indicate, however, that

ATI-5261 retained high α-helical content over a broad range of concentrations (6—310 μM). This includes several independent experiments using ATI-5261 at concentrations as little as 18 μg/mL (lowest concentration currently tested), where the monomeric form of the peptide is produced and saturation of cholesterol efflux is expected. This may explain the potent cholesterol efflux activity of ATI-5261, as secondary structure is thought to be a key determinant for mediating ABCA1 cholesterol efflux.[35,52] Moreover, the absence of end-group capping or presence of membrane mimetic TFE had little impact on secondary structure, indicating ATI-5261 exhibited a strong propensity to adopt an α-helix conformation. The former also indicates that an α-helical content of at least 50—60% is sufficient to stimulate cellular cholesterol efflux efficiently. The lack of strict dependence of ATI-5261 α-helical content on concentration further suggests that intramolecular forces may influence secondary structure and activity. Thus, it is likely the primary amino acid sequence of ATI-5261 greatly favors formation of secondary structure and, perhaps, self-association and solubility properties.

The molecular features of ATI-5261 that govern self-association are currently not known. However, this could involve numerous factors such as peptide size, charge, and/or hydrophobic residues, which direct peptide—peptide interactions. This is supported by data derived from SAXS and tryptophan flourescence, whereby the ATI-5261 oligomer appears to adopt a unique shape with distinct features toward the ends and central regions. Also noteworthy is that ATI-5261 was derived from a segment of apoE that possesses reasonable good secondary structure and self-association properties,[39,53] suggesting that putative determinants governing

formation of the tetrameric assembly may be inherent to sequences from which the peptide was derived. Although speculative, increased secondary structure may also play a role minimizing potential for nonspecific or random interactions (i.e., aggregation tendency) between peptide molecules.

In summary, ATI-5261 represents a novel HDL/apolipoprotein mimetic with greatly improved drugability features, such as high aqueous solubility and limited aggregation tendency. Additional noteworthy features include ability to adopt a specific tertiary form in solution composed of a limited number of α-helical peptide strands as well as high α-helical content upon dilution, i.e., in the absence of lipid. These features may enable more detailed structural analysis, providing models to make further design improvements and/or platforms for creating highly efficient cholesterol efflux peptides. Thus, ATI-5261 appears to constitute an attractive new model to define structure—activity relationships and antiatherosclerosis mechanisms. Such a model takes into account oligomerization/dissociation behavior and secondary structure of peptide monomers. A deeper understanding of apolipoprotein self-association/dynamics may prove useful for optimizing overall structure and translatability of HDL/apolipoprotein mimetic therapies.

■ AUTHOR INFORMATION

Corresponding Author
*Phone: 510-495-2208. Fax: 510-486-6488. E-mail: jkbielicki@lbl.gov.

Author Contributions
⊥The first two authors contributed equally to this work.

■ ACKNOWLEDGMENT

■ ABBREVIATIONS

SAXS, small-angle X-ray scattering; Apo, apolipoprotein; RCT, reverse cholesterol transport; FPLC, fast protein liquid chromatography; DMS, dimethyl suberimidate; CD, circular dichroism; TFE, trifluoroethanol; FBS, fetal bovine serum; BSA, bovine serum albumin; DMPC, dimyristoylphosphatidylcholine; LMW, low molecular weight; HMW, high molecular weight.

■ REFERENCES

(1) Segrest, J. P., Li, L., Anantharamaiah, G. M., Harvey, S. C., Liadaki, K. N., and Zannis, V. (2000) Structure and function of apolipoprotein A-I and high-density lipoprotein. *Curr. Opin. Lipidol. 11*, 105–115.

(2) Gordon, T., Castelli, W. P., Hjortland, M. C., Kannel, W. B., and Dawber, T. R. (1977) High density lipoprotein as a protective factor against coronary heart disease. The Framingham Study. *Am. J. Med. 62*, 707–714.

(3) Rifkind, B. M. (1990) High-density lipoprotein cholesterol and coronary artery disease: survey of the evidence. *Am. J. Cardiol. 66*, 3A–6A.

(4) Ajees, A. A., Anantharamaiah, G. M., Mishra, V. K., Hussain, M. M., and Murthy, H. M. (2006) Crystal structure of human apolipoprotein A-I: insights into its protective effect against cardiovascular diseases. *Proc. Natl. Acad. Sci. U.S.A. 103*, 2126–2131.

(5) Vaisar, T., Pennathur, S., Green, P. S., Gharib, S. A., Hoofnagle, A. N., Cheung, M. C., Byun, J., Vuletic, S., Kassim, S., Singh, P., Chea, H., Knopp, R. H., Brunzell, J., Geary, R., Chait, A., Zhao, X. Q., Elkon, K., Marcovina, S., Ridker, P., Oram, J. F., and Heinecke, J. W. (2007) Shotgun proteomics implicates protease inhibition and complement activation in the antiinflammatory properties of HDL. *J. Clin. Invest. 117*, 746–756.

(6) Ladu, M. J., Reardon, C., Van Eldik, L., Fagan, A. M., Bu, G., Holtzman, D., and Getz, G. S. (2000) Lipoproteins in the central nervous system. *Ann. N.Y. Acad. Sci. 903*, 167–175.

(7) Wilhelm, A. J., Zabalawi, M., Grayson, J. M., Weant, A. E., Major, A. S., Owen, J., Bharadwaj, M., Walzem, R., Chan, L., Oka, K., Thomas, M. J., and Sorci-Thomas, M. G. (2009) Apolipoprotein A-I and its role in lymphocyte cholesterol homeostasis and autoimmunity. *Arterioscler. Thromb. Vasc. Biol. 29*, 843–849.

(8) Kattan, O. M., Kasravi, F. B., Elford, E. L., Schell, M. T., and Harris, H. W. (2008) Apolipoprotein E-mediated immune regulation in sepsis. *J. Immunol. 181*, 1399–1408.

(9) Smith, J. D. (2000) Apolipoprotein E4: an allele associated with many diseases. *Ann. Med. 32*, 118–127.

(10) Strittmatter, W. J., and Roses, A. D. (1995) Apolipoprotein E and Alzheimer disease. *Proc. Natl. Acad. Sci. U.S.A. 92*, 4725–4727.

(11) Rubin, E. M., Krauss, R. M., Spangler, E. A., Verstuyft, J. G., and Clift, S. M. (1991) Inhibition of early atherogenesis in transgenic mice by human apolipoprotein AI. *Nature 353*, 265–267.

(12) Tangirala, R. K., Tsukamoto, K., Chun, S. H., Usher, D., Pure, E., and Rader, D. J. (1999) Regression of atherosclerosis induced by liver-directed gene transfer of apolipoprotein A-I in mice. *Circulation 100*, 1816–1822.

(13) Linsel-Nitschke, P., and Tall, A. R. (2005) HDL as a target in the treatment of atherosclerotic cardiovascular disease. *Nat. Rev. Drug Discovery 4*, 193–205.

(14) Navab, M., Anantharamaiah, G. M., Reddy, S. T., Van Lenten, B. J., and Fogelman, A. M. (2009) HDL as a biomarker, potential therapeutic target, and therapy. *Diabetes 58*, 2711–2717.

(15) Bellosta, S., Mahley, R. W., Sanan, D. A., Murata, J., Newland, D. L., Taylor, J. M., and Pitas, R. E. (1995) Macrophage-specific expression of human apolipoprotein E reduces atherosclerosis in hypercholesterolemic apolipoprotein E-null mice. *J. Clin. Invest. 96*, 2170–2179.

(16) Greenow, K., Pearce, N. J., and Ramji, D. P. (2005) The key role of apolipoprotein E in atherosclerosis. *J. Mol. Med. 83*, 329–342.

(17) Davignon, J., Cohn, J. S., Mabile, L., and Bernier, L. (1999) Apolipoprotein E and atherosclerosis: insight from animal and human studies. *Clin. Chim. Acta 286*, 115–143.

(18) Rothblat, G. H., Bamberger, M., and Phillips, M. C. (1986) Reverse cholesterol transport. *Methods Enzymol. 129*, 628–644.

(19) Fielding, C. J., and Fielding, P. E. (1995) Molecular physiology of reverse cholesterol transport. *J. Lipid Res. 36*, 211–228.

(20) Tall, A. R. (1998) An overview of reverse cholesterol transport. *Eur. Heart J. 19* (Suppl. A), A31–35.

(21) Zhang, Y., Zanotti, I., Reilly, M. P., Glick, J. M., Rothblat, G. H., and Rader, D. J. (2003) Overexpression of apolipoprotein A-I promotes reverse transport of cholesterol from macrophages to feces in vivo. *Circulation 108*, 661–663.

(22) Lewis, G. F., and Rader, D. J. (2005) New insights into the regulation of HDL metabolism and reverse cholesterol transport. *Circ. Res. 96*, 1221–1232.

(23) Rothblat, G. H., and Phillips, M. C. (2010) High-density lipoprotein heterogeneity and function in reverse cholesterol transport. *Curr. Opin. Lipidol. 21*, 229–238.

(24) Bookheimer, S., and Burggren, A. (2009) APOE-4 genotype and neurophysiological vulnerability to Alzheimer's and cognitive aging. *Annu. Rev. Clin. Psychol. 5*, 343–362.

(25) Kim, J., Basak, J. M., and Holtzman, D. M. (2009) The role of apolipoprotein E in Alzheimer's disease. *Neuron 63*, 287–303.

(26) Bu, G. (2009) Apolipoprotein E and its receptors in Alzheimer's disease: pathways, pathogenesis and therapy. *Nat. Rev. Neurosci. 10*, 333–344.

(27) Tardif, J. C., Gregoire, J., L'Allier, P. L., Ibrahim, R., Lesperance, J., Heinonen, T. M., Kouz, S., Berry, C., Basser, R., Lavoie, M. A., Guertin, M. C., and Rodes-Cabau, J. (2007) Effects of reconstituted high-density lipoprotein infusions on coronary atherosclerosis: a randomized controlled trial. *JAMA, J. Am. Med. Assoc. 297*, 1675–1682.

(28) Tardif, J. C., Heinonen, T., and Noble, S. (2009) High-density lipoprotein/apolipoprotein A-I infusion therapy. *Curr. Atheroscler. Rep. 11*, 58–63.

(29) Shah, P. K., Nilsson, J., Kaul, S., Fishbein, M. C., Ageland, H., Hamsten, A., Johansson, J., Karpe, F., and Cercek, B. (1998) Effects of recombinant apolipoprotein A-I(Milano) on aortic atherosclerosis in apolipoprotein E-deficient mice. *Circulation 97*, 780–785.

(30) Alexander, E. T., Weibel, G. L., Joshi, M. R., Vedhachalam, C., de la Llera-Moya, M., Rothblat, G. H., Phillips, M. C., and Rader, D. J. (2009) Macrophage reverse cholesterol transport in mice expressing ApoA-I Milano. *Arterioscler. Thromb. Vasc. Biol. 29*, 1496–1501.

(31) Nissen, S. E., Tsunoda, T., Tuzcu, E. M., Schoenhagen, P., Cooper, C. J., Yasin, M., Eaton, G. M., Lauer, M. A., Sheldon, W. S., Grines, C. L., Halpern, S., Crowe, T., Blankenship, J. C., and Kerensky, R. (2003) Effect of recombinant ApoA-I Milano on coronary atherosclerosis in patients with acute coronary syndromes: a randomized controlled trial. *JAMA, J. Am. Med. Assoc. 290*, 2292–2300.

(32) Shah, P. K. (2007) Apolipoprotein A-I/HDL infusion therapy for plaque stabilization-regression: a novel therapeutic approach. *Curr. Pharm. Des. 13*, 1031–1038.

(33) Vedhachalam, C., Narayanaswami, V., Neto, N., Forte, T. M., Phillips, M. C., Lund-Katz, S., and Bielicki, J. K. (2007) The C-terminal lipid-binding domain of apolipoprotein E is a highly efficient mediator of ABCA1-dependent cholesterol efflux that promotes the assembly of high-density lipoproteins. *Biochemistry 46*, 2583–2593.

(34) Wool, G. D., Vaisar, T., Reardon, C. A., and Getz, G. S. (2009) An apoA-I mimetic peptide containing a proline residue has greater in vivo HDL binding and anti-inflammatory ability than the 4F peptide. *J. Lipid Res. 50*, 1889–1900.

(35) Yancey, P. G., Bielicki, J. K., Johnson, W. J., Lund-Katz, S., Palgunachari, M. N., Anantharamaiah, G. M., Segrest, J. P., Phillips, M. C., and Rothblat, G. H. (1995) Efflux of cellular cholesterol and phospholipid to lipid-free apolipoproteins and class A amphipathic peptides. *Biochemistry 34*, 7955–7965.

(36) Gillotte, K. L., Zaiou, M., Lund-Katz, S., Anantharamaiah, G. M., Holvoet, P., Dhoest, A., Palgunachari, M. N., Segrest, J. P., Weisgraber, K. H., Rothblat, G. H., and Phillips, M. C. (1999) Apolipoprotein-mediated plasma membrane microsolubilization. Role of lipid affinity and membrane penetration in the efflux of cellular cholesterol and phospholipid. *J. Biol. Chem. 274*, 2021–2028.

(37) Walensky, L. D., Kung, A. L., Escher, I., Malia, T. J., Barbuto, S., Wright, R. D., Wagner, G., Verdine, G. L., and Korsmeyer, S. J. (2004) Activation of apoptosis in vivo by a hydrocarbon-stapled BH3 helix. *Science 305*, 1466–1470.

(38) Datta, G., Chaddha, M., Hama, S., Navab, M., Fogelman, A. M., Garber, D. W., Mishra, V. K., Epand, R. M., Epand, R. F., Lund-Katz, S., Phillips, M. C., Segrest, J. P., and Anantharamaiah, G. M. (2001) Effects of increasing hydrophobicity on the physical-chemical and biological properties of a class A amphipathic helical peptide. *J. Lipid Res. 42*, 1096–1104.

(39) Bielicki, J. K., Zhang, H., Cortez, Y., Zheng, Y., Narayanaswami, V., Patel, A., Johansson, J., and Azhar, S. (2010) A new HDL mimetic peptide that stimulates cellular cholesterol efflux with high efficiency greatly reduces atherosclerosis in mice. *J. Lipid Res. 51*, 1496–1503.

(40) Vitello, L. B., and Scanu, A. M. (1976) Studies on human serum high density lipoproteins. Self-association of apolipoprotein A-I in aqueous solutions. *J. Biol. Chem. 251*, 1131–1136.

(41) Ren, X., Zhao, L., Sivashanmugam, A., Miao, Y., Korando, L., Yang, Z., Reardon, C. A., Getz, G. S., Brouillette, C. G., Jerome, W. G., and Wang, J. (2005) Engineering mouse apolipoprotein A-I into a monomeric, active protein useful for structural determination. *Biochemistry 44*, 14907–14919.

(42) Van Lenten, B. J., Wagner, A. C., Anantharamaiah, G. M., Navab, M., Reddy, S. T., Buga, G. M., and Fogelman, A. M. (2009) Apolipoprotein A-I mimetic peptides. *Curr. Atheroscler. Rep. 11*, 52–57.

(43) Navab, M., Anantharamaiah, G. M., Reddy, S. T., Hama, S., Hough, G., Grijalva, V. R., Yu, N., Ansell, B. J., Datta, G., Garber, D. W., and Fogelman, A. M. (2005) Apolipoprotein A-I mimetic peptides. *Arterioscler. Thromb. Vasc. Biol. 25*, 1325–1331.

(44) Hura, G. L., Menon, A. L., Hammel, M., Rambo, R. P., Poole, F. L., II, Tsutakawa, S. E., Jenney, F. E., Jr., Classen, S., Frankel, K. A., Hopkins, R. C., Yang, S. J., Scott, J. W., Dillard, B. D., Adams, M. W., and Tainer, J. A. (2009) Robust, high-throughput solution structural analyses by small angle X-ray scattering (SAXS). *Nat. Methods 6*, 606–612.

(45) Svergun, D. I. (1999) Restoring low resolution structure of biological macromolecules from solution scattering using simulated annealing. *Biophys. J. 76*, 2879–2886.

(46) Patel, A. B., Khumsupan, P., and Narayanaswami, V. (2010) Pyrene fluorescence analysis offers new insights into the conformation of the lipoprotein-binding domain of human apolipoprotein E. *Biochemistry 49*, 1766–1775.

(47) Natarajan, P., Forte, T. M., Chu, B., Phillips, M. C., Oram, J. F., and Bielicki, J. K. (2004) Identification of an apolipoprotein A-I structural element that mediates cellular cholesterol efflux and stabilizes ATP binding cassette transporter A1. *J. Biol. Chem. 279*, 24044–24052.

(48) Choy, N., Raussens, V., and Narayanaswami, V. (2003) Intermolecular coiled-coil formation in human apolipoprotein E C-terminal domain. *J. Mol. Biol. 334*, 527–539.

(49) Chroni, A., Pyrpassopoulos, S., Thanassoulas, A., Nounesis, G., Zannis, V. I., and Stratikos, E. (2008) Biophysical analysis of progressive C-terminal truncations of human apolipoprotein E4: insights into secondary structure and unfolding properties. *Biochemistry 47*, 9071–9080.

(50) Datta, G., Epand, R. F., Epand, R. M., Chaddha, M., Kirksey, M. A., Garber, D. W., Lund-Katz, S., Phillips, M. C., Hama, S., Navab, M., Fogelman, A. M., Palgunachari, M. N., Segrest, J. P., and Anantharamaiah, G. M. (2004) Aromatic residue position on the nonpolar face of class a amphipathic helical peptides determines biological activity. *J. Biol. Chem. 279*, 26509–26517.

(51) Garai, K., and Frieden, C. (2010) The Association-Dissociation Behavior of the ApoE Proteins: Kinetic and Equilibrium Studies. *Biochemistry 49*, 9533–9541.

(52) Brubaker, G., Peng, D. Q., Somerlot, B., Abdollahian, D. J., and Smith, J. D. (2006) Apolipoprotein A-I lysine modification: effects on helical content, lipid binding and cholesterol acceptor activity. *Biochim. Biophys. Acta 1761*, 64–72.

(53) Aggerbeck, L. P., Wetterau, J. R., Weisgraber, K. H., Wu, C. S., and Lindgren, F. T. (1998) Human apolipoprotein E3 in aqueous solution. II. Properties of the amino- and carboxyl-terminal domains. *J. Biol. Chem. 263*, 6249–6258.